THE ASTROPHYSICAL JOURNAL, 554:684–693, 2001 June 20
© 2001. The American Astronomical Society. All rights reserved. Printed in U.S.A.

ON THE CONTRIBUTION OF UNRESOLVED GALACTIC STARS TO THE DIFFUSE SOFT X-RAY BACKGROUND

K. D. KUNTZ[1,2]
Department of Astronomy, University of Maryland, College Park, MD 20742; kuntz@astro.umd.edu
AND
S. L. SNOWDEN[3]
NASA Goddard Space Flight Center, Laboratory for High Energy Astrophysics, Code 662, Greenbelt, MD 20771; snowden@lheavx.gsfc.nasa.gov
Received 2000 December 29; accepted 2001 February 14

ABSTRACT

Using stellar luminosity functions derived from *ROSAT* data, the contributions of Galactic stars to the diffuse X-ray background are calculated for *ROSAT* PSPC energy bands. The model follows that of Guillout and coworkers but uses *ROSAT* rather than *Einstein* data to determine the intrinsic luminosity distributions. The model adequately predicts the numbers of stellar sources observed in deep *ROSAT* surveys. The contribution of unresolved stellar sources to the *ROSAT* All-Sky Survey at the Galactic poles is 6.85, 4.76, and 4.91×10^{-6} counts s^{-1} $arcmin^{-2}$ in bands R12 ($\frac{1}{4}$ keV), R45 ($\frac{3}{4}$ keV), and R67 (1.5 keV), respectively, which is equivalent to 4.66, 31.3, and 26.9×10^{-14} ergs cm^{-2} s^{-1} deg^{-2}.

Subject headings: X-rays: diffuse background — X-rays: ISM — X-rays: stars

1. INTRODUCTION

1.1. *Motivation*

Recent advances in the study of the soft X-ray background have attempted to place limits on the amount of emission from diffuse extragalactic sources. Cen & Ostriker (1999) suggested that such a background might exist in the $\frac{1}{4}$ and $\frac{3}{4}$ keV ranges as a result of gas accretion on subcluster-size objects forming filamentary structures on cosmological scales, the exact form of these structures being sensitive to the cosmological model. At higher energies (above ~ 1 keV), truly diffuse extragalactic X-ray emission is ruled out since such gas would produce unacceptably large perturbations in the microwave background (Wright et al. 1994). Such considerations do not hold at $\frac{1}{4}$ keV, but the multiplicity of backgrounds (at least two diffuse Galactic backgrounds, as well as unresolved Galactic point sources and unresolved extragalactic sources) make the detection of a diffuse extragalactic background difficult. *ROSAT* observations have been used to attack the problem on several different fronts.

The extragalactic background due to unresolved point sources can be characterized as a power law at $E > 1$ keV, and a variety of results, including recent *Chandra* observations (Mushotzky et al. 2000), suggest that this power law extends, without a break, to lower energies. Snowden et al. (2000) and Kuntz & Snowden (2000), following the work of Snowden et al. (1998), have studied the emission that is not due to unresolved extragalactic sources. Snowden et al. (1998) separated the $\frac{1}{4}$ keV emission originating from beyond the Galactic absorption from that due to the Local Hot Bubble, and this work was extended by Kuntz & Snowden (2000) to the remainder of the *ROSAT* band. Although Kuntz & Snowden (2000) characterized the emission originating beyond the Galactic absorption in the $\frac{3}{4}$ keV band, they were not able to effect a separation of the emission from beyond the Galactic absorption into its various components: the Galactic halo, the diffuse extragalactic emission, and unresolved Galactic point sources. Thus, although there is almost no doubt that there is a Galactic halo, the upper limit to the diffuse extragalactic emission in the $\frac{3}{4}$ keV band remains the total emission originating beyond the Galactic absorption. Included in the measure of the emission originating beyond the Galactic absorption was the bulk of the contribution due to unresolved Galactic point sources. It is thus necessary to calculate that contribution to further tighten the limits on the diffuse extragalactic background.

From the model of Cen & Ostriker (1999), the diffuse extragalactic background will not be smooth, and the clumpiness is a function of the cosmological model. Kuntz (2000) sought to place limits on the spatial fluctuations that might be due to the diffuse extragalactic background, and thus it was necessary to determine the degree of fluctuation due to unresolved Galactic point sources.

It is thus particularly interesting for the study of the diffuse extragalactic background to study the luminosity function of Galactic point sources, which, at high Galactic latitudes, are stars.

1.2. *Previous Work*

A stellar log N– log S relation in the form of a cumulative luminosity function (CLF; the number of sources, N, with fluxes greater than S) has been calculated by Guillout et al. (1996) from a mixture of *Einstein* IPC and *ROSAT* PSPC data, using the Bienaymé, Robin, & Crézé (1987) model of the spatial distribution of stars. The Guillout et al. (1996) study concentrated on comparing the model distribution of stellar sources with observed count rates as a function of position, the complement of the information required for studies of the diffuse X-ray background.

There are a number of difficulties in applying the published Guillout et al. (1996) CLF to the problem of unresolved stellar sources. First, the Guillout et al. (1996) study published the CLF for the entire *ROSAT* PSPC bandpass. Since the angular structure of the diffuse X-ray background is strongly energy dependent, studies of the diffuse X-ray background are generally confined to only

[1] Mailing address: NASA Goddard Space Flight Center, Laboratory for High Energy Astrophysics, Code 662, Greenbelt, MD 20771.
[2] Current institution: Department of Physics, University of Maryland, Baltimore County, 1000 Hilltop Circle, Baltimore, MD 21250.
[3] Universities Space Research Association.

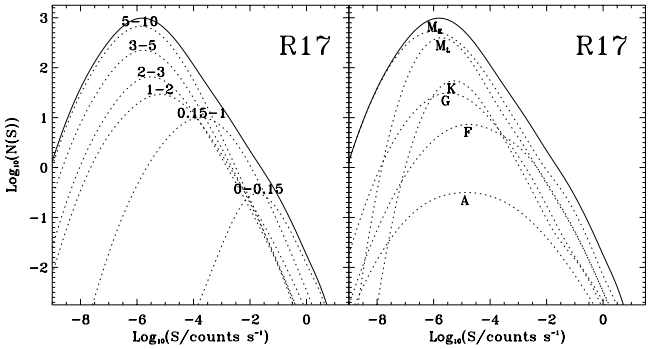


FIG. 1.—Luminosity function, $N(S)d\log S$, for band R17 shown with the fractional contributions of the different age classes (*left*) and spectral types (*right*).

some portion of that bandpass. Given the strong differences in the absorption by the interstellar medium (ISM) from one end of the bandpass to the other, no simple scaling can be applied to the published relations to obtain the relation for any subband. Second, as can be seen in Guillout et al. (1996), and again in our Figure 1, although older stars have lower X-ray luminosities, they form such a large fraction of the total stellar population that they dominate the luminosity function, especially at lower flux levels. However, this is the population that is the least well characterized in the Guillout et al. (1996) study; they were forced to take data from *Einstein* IPC studies of field stars. Far superior *ROSAT* studies have since become available (Schmitt, Fleming, & Giampapa 1995; Schmitt 1997).

The following model calculation uses the best current data to derive the luminosity function at high Galactic latitude, which will be of greatest interest to those studying the diffuse extragalactic background. Rather than the CLF, we calculate the more useful form,

$$N(S)d\log S\,, \tag{1}$$

which allows the calculation of

$$\int_0^{S'} SN(S)d\log S\,, \tag{2}$$

the flux in unresolved sources. The model is, in principle, capable of calculating the stellar contribution at low Galactic latitudes, but some poorly determined input parameters, such as the intrinsic luminosity probability distribution for young stars, greatly increase the uncertainties near the Galactic plane. The irregularity of the spatial distribution of the ISM also introduces some uncertainty, more in softer bands than in harder and more at lower Galactic latitudes.

2. DATA

In order to calculate the contribution of stellar sources, the stellar populations were binned by spectral type $\mathscr{S}_T$ and age $\mathscr{A}$. We used the spectral-type divisions of Schmitt et al. (1995) and Schmitt (1997) and the age divisions of Guillout et al. (1996), all of which are listed in Table 1. The division by age is as follows: the 0–0.15 Gyr class is represented by the Pleiades (171 *ROSAT*-detected members, $\sim$0.1 Gyr, 127 pc), the 0.15–1.0 Gyr class is represented by the Hyades (191 detected members, $\sim$0.6 Gyr, 45 pc), and the 1.0–10.0 Gyr class is represented by the field population.

The data are insufficient to determine the X-ray luminosity functions for subsamples of the 1–10 Gyr field population, which, especially for the later type stars, will be nearly uniformly distributed through the age range. However, stars in the 1–2 Gyr age range will have a very different z-height distribution from stars in the 5–10 Gyr age range. Thus, for calculation, the stars in the 1–10 Gyr age class are subdivided into the age ranges used by Bienaymé et al. (1987; see Table 2), although the same X-ray luminosity function is used for all the age subdivisions in the 1–10 Gyr age class.

Other well-studied clusters could be included with the Hyades for a sample of stars in the 0.15–1.0 Gyr group: Coma Berenices (42 detected members, $\sim$0.5 Gyr, 80 pc) and Praesepe (56 detected members, $\sim$0.6 Gyr, 160 pc). X-ray emission from Coma Berenices members is similar to that from Hyades members (Randich, Schmitt, & Prosser 1996), while that from Praesepe members is lower than that from (coeval) Hyades members (Randich & Schmitt 1995). Given that the Hyades would seem to be representative of its age class and that there is a relatively larger sample available from the Hyades cluster than from other clusters, the other clusters have not been included in this age class. However, it should be borne in mind that the Hyades luminosities may need to be adjusted downward to truly represent its age class.

Although X-ray emission has been detected from nearly every spectral type, the dominant contribution by stellar sources is from low-mass main-sequence dwarfs, due to both intrinsic luminosity and the number of sources.

Stars of spectral type A have been excluded from the model. The intrinsic X-ray luminosity probability distribution is poorly determined for the younger age classes and is currently undetermined for the 1–10 Gyr age class, which would dominate the emission from the A spectral type. The intrinsic X-ray luminosities, where measurable, are about an order of magnitude below those of F stars, and the midplane number density is lower than that of F stars by a factor of 0.005 for the 1–10 Gyr age class. Since the younger age classes will have low z-heights, the error introduced will be minimal for high Galactic latitudes. Guillout et al. (1996) estimate the maximum contribution from A stars to be $\sim$2%.

White dwarfs have also been excluded from the calculation since their contributions are typically 2 orders of magnitude below that of main-sequence stars in the $\frac{1}{4}$ keV band and significantly lower in the $\frac{3}{4}$ and 1.5 keV bands.

RS CVn systems have also been excluded from the calculation. Although they have high luminosities (the median intrinsic luminosity is $\log L_X \sim 30.3$; here, as in the remainder of this paper, L_X is in units of ergs s^{-1} in the 0.1–2.4 keV band; Dempsey et al. 1993), their number density is quite low, probably less than 1×10^{-4} pc^{-3} (Ottmann & Schmitt 1992) as is their scale height ($\sim$325 pc). At high Galactic latitudes, any RS CVn system is likely to be close enough to be detected and not contribute to the "diffuse" background. Giants and supergiants have been excluded from the calculation since their proper calculation would require extensive analysis beyond the scope of this paper. Nearly all giants earlier than K3 are X-ray sources with $\log L_X \sim 27.3$, similar to solar-type stars (Schröder, Hünsch, & Schmitt 1998; Hünsch et al. 1998), but the source population is much smaller and more closely restricted to the plane.

We have also excluded Population II stars from the calculation. If a comparison between disk RS CVn systems and Population II binaries is any indication of the relative emis-

TABLE 1

STELLAR DATA

TYPE	$B-V$	M_V	0–0.15 Gyr[a] Number[d]	0–0.15 Gyr[a] μ[e]	0–0.15 Gyr[a] σ[e]	0.15–1 Gyr[b] Number[d]	0.15–1 Gyr[b] μ[e]	0.15–1 Gyr[b] σ[e]	1–10 Gyr[c] Number[d]	1–10 Gyr[c] μ[e,f]	1–10 Gyr[c] σ[e,f]
A[g]	−0.01–0.29	...	16/39	28.51 ± 0.26	0.99 ± 0.16	10/35	27.84 ± 0.39	0.93 ± 0.29	16/62[h]	...	...
F	0.3–0.6	...	30/33	29.39 ± 0.07	0.32 ± 0.06	57/60	28.93 ± 0.05	0.28 ± 0.03	28/29	28.00 ± 0.14	0.96 ± 0.14
G	0.61–0.8	...	19/26	29.39 ± 0.20	0.67 ± 0.18	27/33	28.64 ± 0.12	0.39 ± 0.05	29/38	27.36 ± 0.17	0.82 ± 0.13
K	>0.8	<8	40/44	29.46 ± 0.07	0.42 ± 0.04	51/86	28.29 ± 0.06	0.45 ± 0.08	17/17	27.62 ± 0.17	0.48 ± 0.12
M (early).....	>0.8	8–15	44/55	29.19 ± 0.05	0.32 ± 0.04	56/174	27.89 ± 0.14	0.72 ± 0.12	66/78	26.86 ± 0.10	0.77 ± 0.10
M (late)	>0.8	>15	0	29.12[i]	0.49[i]	0	28.20[i]	0.49[i]	16/19	27.22 ± 0.22	0.49 ± 0.24

[a] Spatial distribution: Bienaymé et al. 1987, eq. (A1); stellar sample: Pleiades; data: Stauffer et al. 1994, obtained from pointed PSPC observations.

[b] Spatial distribution: Bienaymé et al. 1987, eq. (A2); stellar sample: Hyades; data: Stern et al. 1995, extracted from RASS, and Pye et al. 1994, obtained from pointed PSPC observations.

[c] Spatial distribution: Bienaymé et al. 1987, eq. (A2); stellar sample: field stars ($d < 13$ pc for F and G stars, $d < 7$ pc for K and M stars); data: Schmitt et al. 1995 and Schmitt 1997, obtained from pointed PSPC observations.

[d] The number of detected stars in the sample divided by the total number of stars in the sample.

[e] The quantities μ and σ are in $\log_{10} L_X$, where L_X is in units of ergs s^{-1} in the 0.1–2.4 keV band. The uncertainties were determined as described in the text.

[f] Since Schmitt 1997 and Schmitt et al. 1995 convert from PSPC counts to luminosity using $(5.30HR + 8.31) \times 10^{-12}$ ergs cm^{-2} s^{-1} (count s^{-1})$^{-1}$, where HR is a hardness ratio, and since HR is luminosity dependent, the σ derived from Schmitt 1997 and Schmitt et al. 1995 data are likely to be systematically larger than those derived from other data sets where the PSPC count-to-luminosity conversion was made with a standard 6×10^{-12} ergs cm^{-2} s^{-1} (count s^{-1})$^{-1}$. This difference in conversion may also introduce a very small offset between these luminosities and those of the other age classes. Our fit values were similar to those of Schmitt et al. 1995 and Schmitt 1997, and we have retained their values.

[g] Spectral-type A is not used in the model calculations. Note the large uncertainties in the parameters of the intrinsic luminosity distribution. The parameters could not be calculated for the field sample as the detected fraction for a sample of main-sequence A stars within 30 pc is $\sim\frac{1}{3}$ and upper limits for the nondetections have not been published.

[h] Number in the RASS Point Source Catalogue (Hünsch et al. 1999). In the $r < 13$ pc sample of Schmitt 1997, there are four A stars, none of which were detected.

[i] Extrapolated from the 1.0–10.0 Gyr class due to lack of data. See text.

TABLE 2

MIDPLANE STELLAR DENSITIES (pc^{-3})

TYPE	AGE GROUP					
	0–0.15 Gyr	0.15–1 Gyr	1–2 Gyr	2–3 Gyr	3–5 Gyr	5–10 Gyr
A	2.16×10^{-4}	3.93×10^{-4}	1.01×10^{-4}	2.55×10^{-7}	0	0
F	2.93×10^{-4}	6.14×10^{-4}	4.40×10^{-4}	2.59×10^{-4}	2.29×10^{-4}	6.99×10^{-5}
G	2.78×10^{-4}	5.82×10^{-4}	4.17×10^{-4}	2.88×10^{-4}	4.39×10^{-4}	9.15×10^{-4}
K	3.31×10^{-4}	6.93×10^{-4}	4.96×10^{-4}	3.42×10^{-4}	5.22×10^{-4}	1.18×10^{-3}
M (early).....	4.28×10^{-3}	8.96×10^{-3}	6.42×10^{-3}	4.43×10^{-3}	6.75×10^{-3}	1.53×10^{-2}
M (late)	2.45×10^{-3}	5.12×10^{-3}	3.67×10^{-3}	2.53×10^{-3}	3.86×10^{-3}	8.73×10^{-3}

NOTES.—Parameter c for each age group: 0–0.15 Gyr, 0.0140; 0.15–1 Gyr, 0.0279; 1–2 Gyr, 0.0457; 2–3 Gyr, 0.0662; 3–5 Gyr, 0.0867; 5–10 Gyr, 0.0958. Parameter c describes the ellipticity of the stellar distribution. See eqs. (A1) and (A2) of Bienaymé et al. 1987.

sion from single Population I and Population II stars, then the Population II stars should have emission that is more than an order of magnitude below that of Population I stars (Ottmann, Fleming, & Pasquini 1997).

2.1. *Model Inputs*

For each spectral-type/age-class bin, the contribution to the luminosity function is determined by four parameters: μ and σ, the mean and dispersion of the intrinsic luminosity probability function, c, which describes the z-distribution of the stars, and n_0, the midplane ($z = 0$) density of stars.

Following Schmitt et al. (1995) and Schmitt (1997), we have assumed that the intrinsic luminosity function for a spectral-type/age-class bin is given by the log-normal distribution,

$$P(\log L_X) = \frac{1}{\sigma\sqrt{2\pi}} \exp -\frac{1}{2}\left(\frac{\log L_X - \mu}{\sigma}\right)^2 . \qquad (3)$$

The parameters $\mu(\mathscr{S}_T, \mathscr{A})$ and $\sigma(\mathscr{S}_T, \mathscr{A})$ were derived from the *ROSAT* data sets listed in Table 1.

Since these data sets contain points with upper limits, the parameters were determined by fitting the Kaplan-Meier estimator (Schmitt 1985) of the cumulative distribution function, where the uncertainty in the Kaplan-Meier estimator was taken from Fiegelson & Nelson (1985). The uncertainties were derived using a bootstrap method (Babu & Feigelson 1996). We corrected for binaries in the same manner as Schmitt et al. (1995): we divided the flux equally between members of binary systems. Guillout et al. (1996) showed that correction for binaries made little difference to the luminosity function.

Since there were no late M stars detected in the surveys of the Hyades or Pleiades, we have extrapolated the μ for the 0–0.15 Gyr and 0.15–1.0 Gyr age classes from the μ for the 1–10 Gyr age class using the general trend observed in the other spectral classes: a $\Delta \log L_X = 0.92$ decrease between the 0–0.15 Gyr and 0.15–1.0 Gyr classes and a $\Delta \log L_X = 0.98$ decrease between the 0.15–1.0 Gyr and 1.0–10.0 Gyr classes. For the late M stars the same value of σ was used for each age class, that of the oldest age class; this tends to increase the number of sources with high fluxes, but not significantly.

To convert from the listed X-ray luminosities to count rates, we used the inverse of the conversion used by the original authors. Stern, Schmitt, & Kahabka (1995) used the conversion 6.0×10^{-12} ergs cm^{-2} s^{-1} (counts $s^{-1})^{-1}$. Stauffer et al. (1994) used a conversion of $\sim 8.4 \times 10^{-12}$ ergs cm^{-2} s^{-1} (counts $s^{-1})^{-1}$ (for $N_H = 0$), characteristic of $\log T = 7.06$. Due to the shape of the conversion curve, this is also the conversion factor for $\log T = 6.88$. Schmitt et al. (1995) used the conversion factor[4] $(5.30HR + 8.31) \times 10^{-12}$ ergs cm^{-2} s^{-1} (counts $s^{-1})^{-1}$, where HR is defined by (R47 − R82)/(R47 + R82) and RXX is the count rate in band XX and the bands are defined in Snowden et al. (1997) and again in Table 3.

From the band R17 count rates, it is neccessary to derive count rates in narrower bands for this study to be of use. To divide the band R17 into the R12 and R47 bands, one can use the $\log L_X$–HR relation developed by J. H. M. M. Schmitt (1998, private communication). Schmitt suggested that for each spectral type, HR is a linear function of the log of the luminosity,

$$\log L_X = aHR + b \; ; \qquad (4)$$

the slopes of these relations seem to be the same for all spectral types, but the intersections are different. The parameters of these relations were determined for the field stars from the data of Schmitt et al. (1995) and Schmitt (1997) by Kuntz (2000).

[4] This relation was derived for a Raymond-Smith model two-component corona fitted to a small number of high signal-to-noise ratio spectra. See Fleming et al. (1995) for a complete description.

TABLE 3

BROADBAND DEFINITIONS

Band	PI Channel	Energy[a] (keV)	Composite Bands
R1	8–19	0.11–0.284	
R1L = R8.....	11–19	0.11–0.284	R12 or R1L2 = $\frac{1}{4}$ keV
R2	20–41	0.14–0.284	
R3	42–51	0.20–0.83	
R4	52–69	0.44–1.01	R45 = $\frac{3}{4}$ keV
R5	70–90	0.56–1.21	
R6	91–131	0.73–1.56	R67 = 1.5 keV
R7	132–201	1.05–2.04	

NOTES.—The notation band RXY denotes the sum of all of the bands between (and including) RX and RY. In the *ROSAT* source catalogs, $HR1$ = (R47 − R12)/(R47 + R12) and $HR2$ = (R67 − R45)/(R67 + R45).

[a] 10% of peak response.

The applicability of these relations to younger stars is not clear. Extracting the Hyades members identified by Stern et al. (1995) from the *ROSAT* Bright and Faint Source Catalogues[5] (Voges et al. 1999), we found that the field star relations fit the Hyades stars well for spectral types F and G. For the M stars, the slopes of the relations appeared consistent, but the field star offsets were too large (i.e., too hard) for the Hyades stars. Since there is a substantial dispersion around the relation for both the field stars and the Hyades and there may be significant biases in the selection of sources for the Bright and Faint Source Catalogues, we have used the field star relations for the younger stars as well. There are not enough Pleiades stars in the Faint Source Catalogue to attempt a similar analysis.

To subdivide the flux further, we investigated the relation between HR and the spectral shape. From the HEASARC archive of *ROSAT* PSPC exposures, we extracted the spectra of all single field dwarfs of spectral classes A through M that had more than $\sim$400 counts, about 16 stars. For these spectra we used XSPEC (Arnaud 1996) to fit two Raymond & Smith (1977) components with temperatures T_S and T_H and normalizations N_S and N_H. We found that the temperature of the softer component, T_S, did not vary with HR ($\log T_S \sim 6.23$), but that for stars in an individual spectral type, the temperature of the harder component, T_H, varied linearly with HR.[6] Given the T_H for a given HR, we then solved for the N_S/N_H ratio that would produce the correct value of HR. This relation between T_H and HR restricts the range of allowable HR to greater than -0.86 and less than 0.37 (for M stars) and less than 0.22 (for F and G stars).

We checked this T_H, N_S/N_H, HR relation against the Hyades stars extracted from the Bright and Faint Source Catalogues using (R47 − R82)/(R47 + R82) versus (R67 − R45)/(R67 + R45) graphs and found that within the large uncertainties of the data, the relations derived from field stars also described the Hyades stars.

Thus, for a given X-ray luminosity, we used the Schmitt relation between the X-ray luminosity and the hardness ratio to determine HR and then used these relations between T_H, N_S/N_H, and HR to derive a spectral energy distribution that can then be used to divide the total number of counts into the counts for each of the *ROSAT* bands. Since the $\log L_X$–HR relation can produce values of HR outside the range allowed by the T_H, N_S/N_H, HR relation, values of HR outside this range were replaced by the closest extreme.

The spatial distribution of each spectral type/age class was assumed to be given by equations (A1) and (A2) of Bienaymé et al. (1987), where $c(\mathscr{A})$, the axial ratio for ellipsoids describing the disk populations, was taken from the "best fit" column of their Table 1 and is listed in a note to our Table 2.

To maintain some consistency between the initial mass function (IMF), the stellar formation rate (SFR), and the relation, the midplane density of each spectral-type/velocity dispersion–age age-class bin, $n_0(\mathscr{S}_T, \mathscr{A})$, was derived in a manner similar to that used by Guillout et al. (1996). The disk was assumed to have an age of 10 Gyr, a constant SFR, and an invariant IMF. The IMF was taken from Haywood, Robin, & Crézé (1997):

$$dN = m^{-(1+x)}\,dm\ , \tag{5}$$

where

$$x = \begin{cases} 0.7 & m < M_\odot\ , \\ 1.5 & 1\ M_\odot \le m < 3\ M_\odot\ , \\ 2.0 & m \ge 3\ M_\odot\ . \end{cases} \tag{6}$$

The total number of stars was normalized by comparing the number produced by the above formula with $r < 7$ pc in the $8 < M_V < 15$ range (i.e., the K and early M stars) with the number actually observed (79). The fraction of the number of stars in each age class was calculated using the main-sequence lifetimes listed in Scalo (1986) and the mass–absolute magnitude–spectral type relations of Kroupa, Tout, & Gilmore (1993).

2.2. *Method*

For each spectral-type/age-class bin, the intrinisic luminosity distribution was evaluated for $\Delta \log L_X = 0.1$ intervals. For each distance interval, $\Delta r = 10$ pc, from 0 to 3000 pc, the value of $\log L_X$ was adjusted for r^{-2} diminution, absorption by the ISM, and converted to count rates in a given band. The probability of finding a star with flux S in a given band, as a function of S, was then interpolated to a standard $\Delta \log (S/\text{counts s}^{-1}) = 0.1$ spacing and scaled by the size of the volume element and the relative stellar density for that z-height. The luminosity function for each spectral type/age class was then summed over the z-height and scaled by the total number of stars.

The vertical distribution of the ISM was taken from Lockman (1984) and was assumed to be plane parallel. The absorption cross sections were taken from Morrison & McCammon (1983). The absorption was calculated using the spectral energy distribution described above. Although the bulk of the stars lies beyond the bulk of the absorption (see Fig. 2), only the R12 band reaches column densities for which $\tau = 1$. (The next most sensitive band is R17, for which $\tau = 1$ at $\sim 5.5 \times 10^{20}$ cm^{-2}.) Thus, the luminosity function is not too sensitive to absorption by the ISM at high Galactic latitudes.

The aggregate luminosity function for band R17 is shown in Figure 1 for the north Galactic pole. As might be expected, the luminosity function is dominated by the older age classes because, although their intrinsic luminosities may be an order of magnitude smaller than the younger age classes, they account for the bulk of the number of sources. For similar reasons, the luminosity function is dominated by the longer lived spectral classes. The high count rate end of the luminosity function is strongly influenced by the younger age classes since they have larger intrinsic luminosities and smaller scale heights.

Figure 3 shows the effect of the uncertainties of the parameters on the luminosity function (*top panel*), unresolved flux (*middle panel*), and cumulative luminosity function (*bottom panel*) for a single spectral type/age class (early M, 1–2 Gyr) in band R47 (the most interesting band for cosmo-

[5] Available at the URLs http://www.xray.mpe.mpg.de/rosat/survey/rass-bsc and http://www.xray.mpe.mpg.de/rosat/survey/rass-fsc.

[6] We found that the F and G stars followed one T_H-HR relation, while the M stars followed another. There were only two K stars in the sample, one of which fell on the relation for F and G stars, the other of which fell between the FG and M relations. Of the M stars, half were dM and half were dMe, so the difference between the FG and M relations is not due to selecting the brighter M stars.

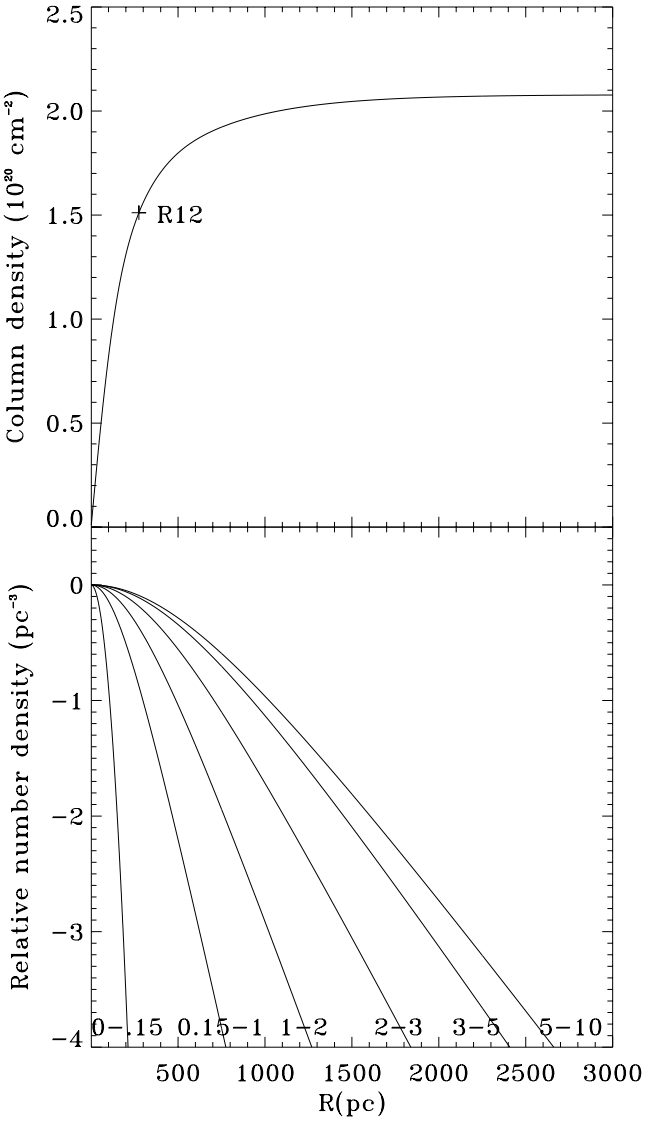


FIG. 2.—Relative number densities for each age group as a function of z-height, compared to the absorbing column through which they are observed. *Top:* The total absorbing column through which an object of z-height R is observed. The $\tau = 1$ point for band R12 is marked; to achieve the same τ for band R47 requires a much greater column density. *Bottom:* The relative number densities for stars of a given age group at a z-height R. Each curve has a midplane number density of unity.

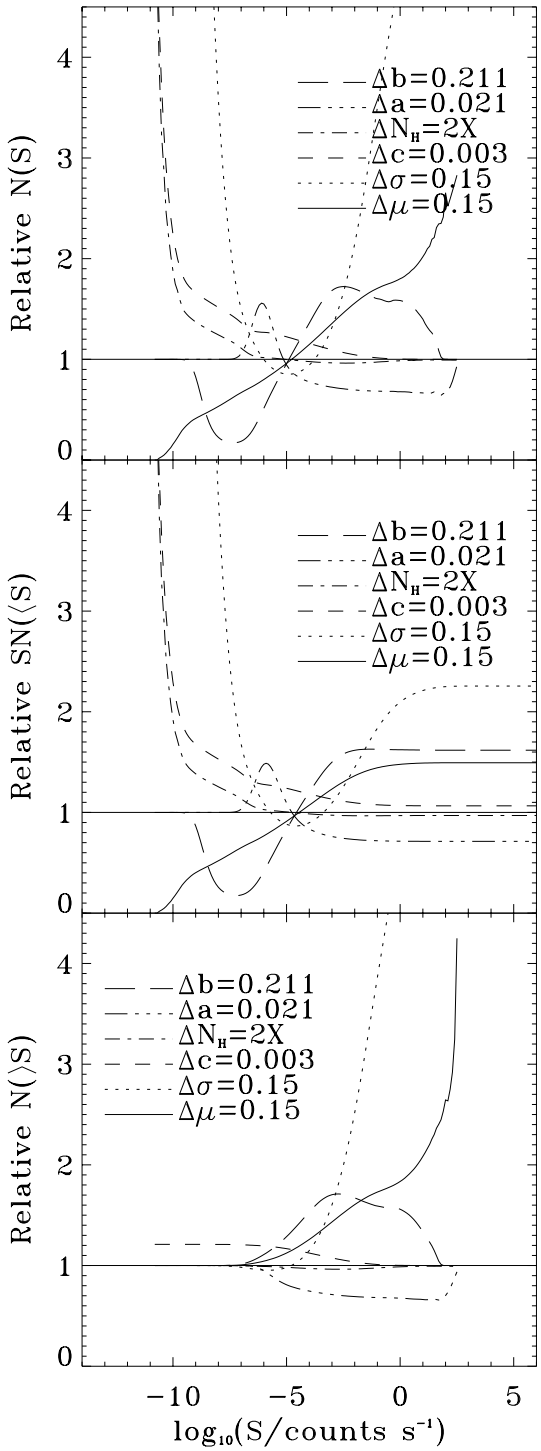


FIG. 3.—Effect of the formal uncertainties of the input parameters on the luminosity function (*top*), the unresolved flux (*middle*), and the cumulative luminosity function (*bottom*) shown as the ratio between the luminosity functions. For the M (early), 1–2 Gyr age class, we show the R47 band luminosity function calculated with a single parameter increased by Δ, where the Δ is the typical formal uncertainty, divided by the fiducial luminosity function.

logical purposes). In this band, the effects of Galactic absorption are minor. The parameter uncertainties are their typical formal uncertainties. For typical survey limits, $-4 < \log S(\mathrm{R47}) < -2$, the predicted unresolved flux is uncertain to a factor of 2 because of the formal uncertainties. The largest sources of uncertainty are the μ and σ of the intrinsic luminosity distribution function. Although the b-paramter of the log L_X–HR relation also appears to contribute a significant uncertainty, the true uncertainty is likely smaller than the value shown here, which includes what may be a significant intrinsic scatter around the relation. Uncertainties in c cause little change.

The true uncertainty in the amount of unresolved flux is much less than that shown in Figure 3: as will be seen, the model can be checked against the observed $N(S)$ over several orders of magnitude in source flux, and good agreement between the model and the observed $N(S)$ implies a smaller error in the unresolved flux.

3. COMPARISONS

The current model agrees fairly well with that of Guillout et al. (1996) except for the late M class. For this class we find

a factor of ~ 10 more sources. Only a small amount of this difference can be attributed to the difference in luminosity distributions: the luminosity distribution used here ($\mu = 27.22$, $\sigma = 0.49$) is surprisingly similar to that derived from *Einstein* data ($\mu = 27.7$, $\sigma \sim 0.42$) by Barbera et al. (1993). It is not clear whether the difference in number counts for the late M class is due to a different IMF, a different low-mass cut-off for X-ray emission ($0.08\ M_\odot$ was used here), or merely a different mass–to–spectral type conversion. All of these quantities are, of course, quite uncertain for the low-mass end of the main sequence.

We have checked our model against the number of stellar point sources found in surveys and against the stellar log N–log S relation of Krautter et al. (1999). These comparisons are listed in Table 4 and shown in Figure 4. The predicted number listed in the table is the number of sources with flux above the survey limit at the (l, b)-position of the survey, per square degree, multiplied by the survey area and the fraction of sources for which identifications have been made (the "ID Completeness").

As can be seen, the model predicts well the band R47 source counts for fluxes below $\log_{10} S \sim -2.5$. At higher fluxes we can compare our model to the wide-field (each field has ~ 144 deg^2) data of Krautter et al. (1999), which is complete in band R17 to 0.03 counts s^{-1} (and thus must be complete to at least that level in the subband R47). We find that in band R47 for their field IVac ($b = 79°$), the model is consistent with observations for fluxes below 0.1 counts s^{-1}. However, below that threshold, the model overpredicts at low latitudes ($30° < |b| < 40°$; their fields I, II, III, and VI). Above this threshold, the model underpredicts the source counts at all latitudes. A similar trend is seen in the band R17 source counts: the model somewhat underpredicts the counts at high Galactic latitudes and overpredicts at low Galactic latitudes for fluxes greater than 0.03 counts s^{-1}. Given the shape of the luminosity functions (Fig. 1), this error is likely due to the poorly determined μ and σ of the youngest age group. (N.B. the caveat given in § 2 concerning the Hyades luminosity function, as well as our use of a log L_X–HR relation for the M stars that may be too hard, decreasing the effect of absorption; § 2.1.)

The problems with the model at bright fluxes do not cast serious doubt on our prediction at lower fluxes: as can be seen from Figure 3, the brighter fluxes are much more sensitive to uncertainties in μ and σ, and the brighter fluxes are much more sensitive to the behavior of the younger age groups. It should also be noted that the uncertainties in the unresolved flux at the brighter fluxes will be significantly smaller than those of the source counts.

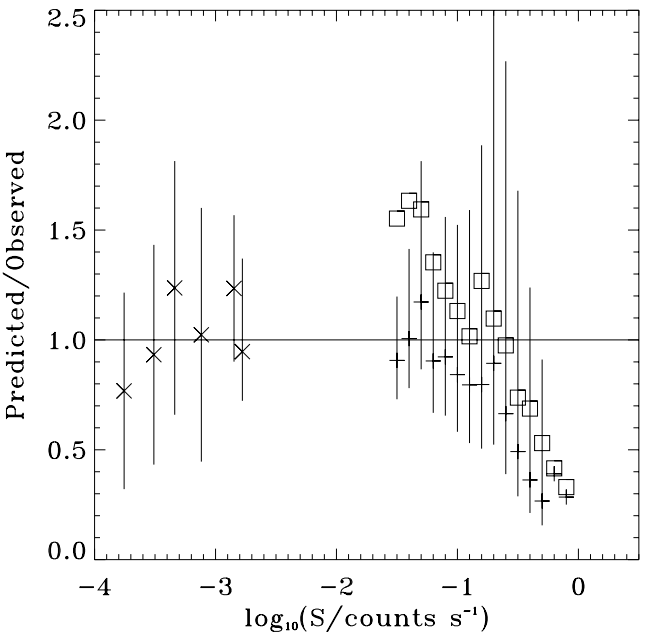


FIG. 4.—Predicted cumulative luminosity function with measured values. *Crosses*: Values in band R47 from the deep surveys listed in Table 4, *plus signs with error bars*: values in band R47 from the field IVac ($b = 79°$) source list of Appenzeller et al. (1998), *open squares, not shown with error bars*: values in band R47 from fields I, II, III, and VI of Appenzeller et al. (1998). These fields have $30° < |b| < 40°$. See text for further explanation.

4. MODEL DESCRIPTION

It is instructive to see how the luminosity function changes with detection band, Galactic latitude, and Galactic longitude.

Figure 5 shows the stellar luminosity function at the north Galactic pole for several *ROSAT* bands. The R12 band is substantially different from the R45 band because of both the different instrumental response (which produces a horizontal shift in the curves) and the differing effects of absorption (which increases the number counts below the

TABLE 4

PREDICTIONS

Survey	(l, b) (2000)	Band	Area (deg^2)	ID Completeness	Source Limit ($\times 10^{-3}$ counts s^{-1})	Number Predicted	Number Found
Bower et al. 1996	(96.4, 29.8)	47	0.21	0.90	0.763	3.07	3
Schmidt et al. 1998	(149.5, 53.5)	47	0.28	1.00	0.459	3.71	3
Zamorani et al. 1999	(270.2, −51.8)	47	0.20	0.84	0.309	3.73	4
McHardy et al. 1998	(85.0, 75.9)	47	0.17	1.00	0.175	3.84	5
Carballo et al. 1995	(162.6, 51.1)	47	2.20	0.57	1.42	11.11	9
Boyle, Wilkes, & Elvis 1997	Various	47	3.92	0.89	1.7	18.93	20
Comparison to Measured log N– log S Function							
Krautter et al. 1999	Various	17			17	0.6[a]	0.64
		17			170	0.058	0.057
		17			1700	0.0032	0.0030

[a] Value from the log N– log S function graphed in their paper. We have assumed that this function is valid for $b = 90°$.

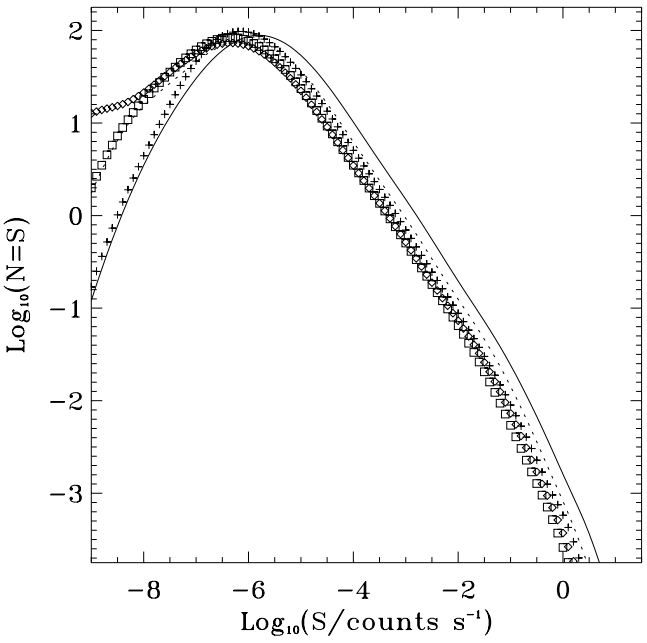


FIG. 5.—Luminosity function for different bands in the direction of the north Galactic pole. *Solid line*: Band R17, *plus signs*: band R12, *open squares*: band R45, *diamonds*: band R67, *dotted line*: band R47 (almost indistinguishable from band R45).

peak and decreases them above the peak, though not at the highest fluxes). The anomolous behavior of band R67 is due to the discontinuity of the $\log L_X$–HR relation at $HR = -0.86$: the rate of decrease of the band R67 flux with decreasing HR is greater than for the other bands, and thus the discontinuity is more pronounced for band R67 than for the other bands. Since the anomolous behavior occurs 2 orders of magnitude below the peak of the luminosity function, it does not cause significant errors.

Figure 6 shows the ratio of the stellar luminosity function at $b = 30°$ to that at the Galactic pole for the R12 and R47 bands. We have assumed a plane-parallel absorption model. For typical deep *ROSAT* surveys, there is a factor of ~ 2.5 greater number of sources at $b = 30°$ than at $b = 90°$ in band R47. The increase in number counts for band R12 is less severe because of absorption. As can be seen from the figure, at $b = 30°$ the effect of the Galactic radial density gradient is negligible.

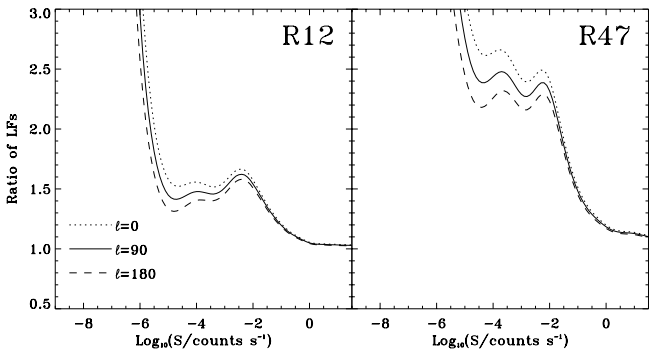


FIG. 6.—Ratio of the luminosity function at $b = 30°$ to the luminosity function at $b = 90°$. *Solid line*: The ratio for $l = 90°$, *dotted line*: the ratio for $l = 0°$, *dashed line*: the ratio for $l = 180°$.

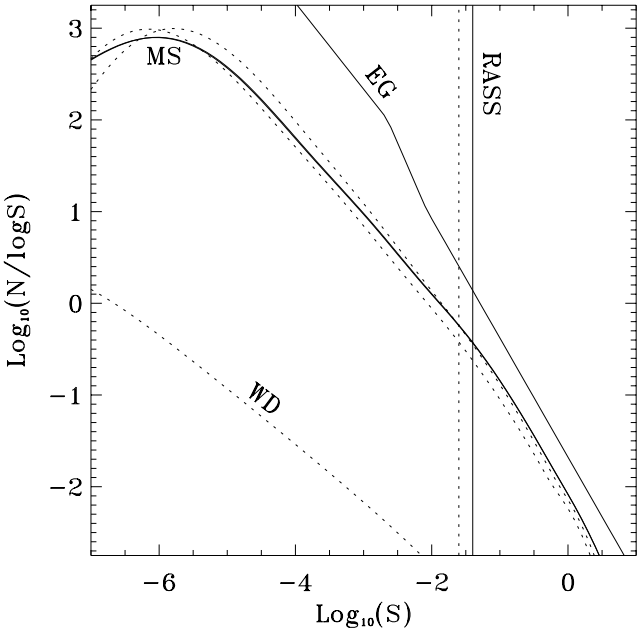


FIG. 7.—Luminosity function for main-sequence stars, white dwarfs, and extragalactic objects, for band R12 (*dotted line*) and band R47 (*solid line*). The relations are shown for a total $N_H = 5 \times 10^{19}$ cm^{-2} (*farther to the right*) and for $N_H = 2.1 \times 10^{20}$ (*farther to the left*). For band R47, the relations for the different values of N_H are indistinguishable. The band R47 relation for white dwarfs is not shown but would be significantly below the R12 relation. The point-source detection limit for the RASS is also shown.

5. RESULTS

Figure 7 shows the luminosity functions in PSPC bands R12 (*dotted lines*) and R47 (*solid lines*) for main-sequence stars, white dwarfs,[7] and the extragalactic luminosity function derived by Hasinger et al. (1998). For band R47, above the *ROSAT* All-Sky Survey (RASS) detection limits, stellar sources account for one-third to one-half of the point sources, in agreement with studies such as those listed in Table 4, while for band R12, the fraction depends upon the total absorbing column.

Figure 8 shows the contribution to the RASS of unresolved stellar sources as a function of Galactic latitude. Table 5 shows the model prediction for the contribution of the unresolved Galactic stars to the diffuse X-ray background at the north Galactic pole for $N_H = 2.1 \times 10^{20}$ cm^{-2}. The conversion of count rates to energy uses the spectral shape of the unresolved flux and the energy ranges listed in the table. At the RASS point-source detection limit in band R45, the unresolved flux has R12:R45:R67 = 1.51:1:1.09, and these ratios are similar for the unresolved flux at the RASS point-source detection limits in the other bands. The unresolved flux in the R47 band (0.44–2.04 keV) is 3.64 and 3.51×10^{-13} ergs cm^{-2} s^{-1} deg^{-2} at the RASS bands R45 and R67 point-source detection limits, respectively.

In bands R12, R45, and R67, the unresolved stellar sources can account for, at most, 2%, 10%, and 51% of the flux that is thought not to be due to the Local Hot Bubble

[7] The white dwarf luminosity function for single white dwarfs is shown to demonstrate its inconsequentiality. It was calculated using the data of Fleming et al. (1996) with the assumption that the intrinsic X-ray luminosity of white dwarfs extends down to at least log $L_X = 27.5$.

TABLE 5

UNRESOLVED STELLAR FLUX

ROSAT BAND	ENERGY RANGE[a] (keV)	RASS PSDL[b] (counts s^{-1})	UNRESOLVED FLUX		
			10^{-6} counts s^{-1} $arcmin^{-2}$	10^{-14} ergs cm^{-2} s^{-1} deg^{-2}	keV cm^{-2} s^{-1} sr^{-1} keV^{-1}
R12.....	0.11–0.284	0.025	6.85	4.66	0.55
R45.....	0.44–1.21	0.02	4.76	31.3	0.83
R67.....	0.73–2.01	0.02	4.91	26.9	0.42

[a] Energy at 10% of the peak response.
[b] Point-source detection limit.

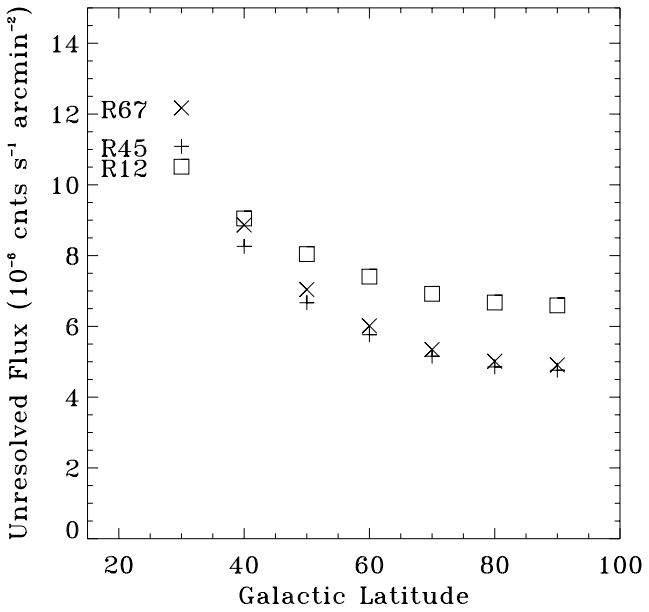


FIG. 8.—Contribution of unresolved stellar sources to the RASS as a function of Galactic latitude. It is assumed that the point-source removal limits were 0.025 counts s^{-1} in band R12 and 0.02 counts s^{-1} in bands R45 and R67.

or the unresolved extragalactic point sources (essentially the component that Kuntz & Snowden 2000 attribute to the Galactic halo but that can be distributed between the Galactic halo and diffuse extragalactic emission). The variation of the contribution from unresolved stellar sources with Galactic latitude would be unnoticeable in the RASS given the uncertainty in the RASS and, more importantly, the variable effects of Galactic absorption.

The deep band R47 surveys discussed in § 3 suggest that the predicted unresolved flux for surveys at high Galactic latitudes with limits $\log S(\mathrm{R47}) < -2.5$ is correct. At higher fluxes the comparison of the model with observations is more equivocal, but the high Galactic latitude source counts in band R47 do seem to be correct (at least for $S \lesssim 0.3$ counts s^{-1}), and thus the unresolved flux should be correct. Because of the uncertainties introduced by the younger stars, the model is not adequate at lower Galactic latitudes ($|b| < 30°$), particularly for the high flux source counts. It should also be noted that both the younger stars and the Galactic absorption will be distributed in a much more clumpy manner than used by this model, so a great deal of field-to-field variation is to be expected.

We would like to thank T. Fleming for several useful discussions about stellar X-ray emission and for his patience as a referee, J. H. M. M. Schmitt for a discussion of the log L_X–HR relation, P. Guillout for guidance on the stellar distribution, and S. Drake for discussions about selection effects in the data from which we constructed our empirical model of the stellar X-ray emission.

REFERENCES

Appenzeller, I., et al. 1998, ApJS, 117, 319
Arnaud, K. A. 1996, in ASP Conf. Ser. 101, Astronomical Data Analysis Software and Systems V, ed. G. Jacoby & J. V. Barnes (San Francisco: ASP), 17
Babu, G. J., & Feigelson, E. D. 1996, Astrostatistics (London: Chapman & Hall)
Barbera, M., Micela, G., Scortino, S., Harnden, F. R., & Rosner, R. 1993, ApJ, 414, 846
Bienaymé, O., Robin, A. C., & Crézé, M. 1987, A&A, 180, 94
Bower, R. G., et al. 1996, MNRAS, 281, 59
Boyle, B. J., Wilkes, B. J., & Elvis, M. 1997, MNRAS, 285, 511
Carballo, R., Warwick, R. S., Barcons, X., Gonzalez-Serrano, J. I., Barber, C. R., Martinez-Gonzalez, E., Peres-Fournon, I., & Burgos, J. 1995, MNRAS, 277, 1312
Cen, R., & Ostriker, J. P. 1999, ApJ, 514, 1
Dempsey, R. C., Linsky, J. L., Fleming, T. A., & Schmitt, J. H. M. M. 1993, ApJS, 86, 599
Fiegelson, E. D., & Nelson, P. I. 1985, ApJ, 293, 192
Fleming, T. A., Molendi, S., Maccacaro, T., & Wolter, A. 1995, ApJS, 99, 701
Fleming, T. A., Snowden, S. L., Pfeffermann, E., Briel, U., & Greiner, J. 1996, A&A, 316, 147
Guillout, P., Haywood, M., Motch, C., & Robin, A. C. 1996, A&A, 316, 89
Hasinger, G., Burg, R., Giacconi, R., Schmidt, M., Trümper, J., & Zamorani, G. 1998, A&A, 329, 482
Haywood, M., Robin, A. C., & Crézé, M. 1997, A&A, 320, 428
Hünsch, M., Schmitt, J. H. M. M., Schröder, K.-P., & Zickgraf, F.-J. 1998, A&A, 330, 225
Hünsch, M., Schmitt, J. H. M. M., Sterzik, M. F., & Voges, W. 1999, A&AS, 135, 319
Krautter, J., et al. 1999, A&A, 350, 743
Kroupa, P., Tout, C. A., & Gilmore, G. 1993, MNRAS, 262, 545
Kuntz, K. D. 2000, Ph.D. thesis, Univ. Maryland
Kuntz, K. D., & Snowden, S. L. 2000, ApJ, 543, 195
Lockman, F. J. 1984, ApJ, 283, 90
McHardy, I. M., et al. 1998, MNRAS, 295, 641
Morrison, R., & McCammon, D. 1983, ApJ, 270, 119
Mushotzky, R. F., Cowie, L. L., Barger, A. J., & Arnaud, K. A. 2000, Nature, 404, 459
Ottmann, R., Fleming, T. A., & Pasquini, L. 1997, A&A, 322, 785
Ottmann, R., & Schmitt, J. H. M. M. 1992, A&A, 256, 421
Pye, J. P., Hodgkin, S. T., Stern, R. A., & Stauffer, J. R. 1994, MNRAS, 266, 798
Randich, S., & Schmitt, J. H. M. M. 1995, A&A, 298, 115
Randich, S., Schmitt, J. H. M. M., & Prosser, C. 1996, A&A, 313, 815
Raymond, J. C., & Smith, B. W. 1977, ApJS, 35, 419

Scalo, J. M. 1986, Fundam. Cosmic Phys., 11, 1
Schmidt, M., et al. 1998, A&A, 329, 495
Schmitt, J. H. M. M. 1985, ApJ, 293, 178
———. 1997, A&A, 318, 215
Schmitt, J. H. M. M., Fleming, T. A., & Giampapa, M. S. 1995, ApJ, 450, 392
Schröder, K.-P., Hünsch, M., & Schmitt, J. H. M. M. 1998, A&A, 335, 591
Snowden, S. L., Egger, R., Finkbeiner, D., Freyberg, M. J., & Plucinsky, P. P. 1998, ApJ, 493, 715
Snowden, S. L., et al. 1997, ApJ, 485, 125
Snowden, S. L., Freyberg, M. J., Kuntz, K. D., & Sanders, W. T. 2000, ApJS, 128, 171
Stauffer, J. R., Caillault, J.-P., Gagné, M., Prosser, C. F., & Hartman, L. W. 1994, ApJS, 91, 625
Stern, R. A., Schmitt, J. H. M. M., & Kahabka, P. T. 1995, ApJ, 448, 683
Voges, W., et al. 1999, A&A, 349, 389
Wright, E. L., et al. 1994, ApJ, 420, 450
Zamorani, G., et al. 1999, A&A, 346, 731